Journal of Materials Chemistry A

Atomic Layer Deposition for Surface Area Determination of Solid Oxide Electrodes

Journal:	*Journal of Materials Chemistry A*
Manuscript ID	TA-ART-11-2022-009060.R1
Article Type:	Paper
Date Submitted by the Author:	22-Jan-2023
Complete List of Authors:	Schmauss, Travis; Northwestern University, Materials Science and Engineering Barnett, Scott; Northwestern University, Materials Science and Engineering

Atomic Layer Deposition for Surface Area Determination of Solid Oxide Electrodes

Travis Schmauss[a] and Scott Barnett[a]

[a] Department of Materials Science and Engineering, Northwestern University, Evanston IL, 60208.

Email: s-barnett@northwestern.edu

Abstract: Surface area measurements are important for characterizing porous solids, but commonly used methods such as Brunauer–Emmett–Teller (BET) gas adsorption and computed nanotomography are lacking for certain applications such as the development of solid oxide fuel cell electrodes, which often have absolute surface areas <1 m^2 and contain nanoscale features. Presented is a novel method for the surface area determination of samples with total measurable areas of 1-1000 cm^2 with a standard deviation ±1 cm^2, utilizing the atomic layer deposition (ALD) of Al_2O_3 over microstructurally complex internal porosity. The volume of alumina is then quantified using plasma spectroscopy and converted to an area using the known ALD layer thickness. Under the modest ALD reactor soak times used (8.5 s), the precursor penetration depth is found to be ~50 μm, exceeding the requirement for uniformly coating SOFC functional layers. A model system, $(La_{0.8}Sr_{0.2})_{0.98}MnO_{3-\delta}$ / $Ce_{0.9}Gd_{0.1}O_{1.95}$ (LSM/GDC) scaffolds of ~2.7 m^2/g, was measured using the technique and compared against the BET method, and comparable results were obtained but with 1,000 times less material needed. The technique is demonstrated for measurements in two example areas of active SOFC research: exsolved (Ni,Fe) nanoparticles on an $Sr(Ti,Fe,Ni)O_{3-\delta}$ electrode and PrO_x catalyst nanoparticles infiltrated onto LSM/GDC scaffolds. The technique may be broadly useful wherever the accurate surface area determination of small absolute quantities of porous ceramic structures on the order of 0.1-50 m^2/g is sought.

Introduction

Surface area determination is a characterization tool that is widely used in the field of heterogeneous and electro- catalysis to quantify normalized activity and performance. For powders and high specific surface area materials (>100 m^2/g) like zeolites and metal-organic frameworks, this need is largely met by the ISO-standard Brunauer, Emmett and Teller (BET) method in which

surface area is calculated from a linear portion of a gas isotherm physisorption experiment. The practical lower limit for absolute total surface area is ~1 m^2 with lower vapor pressure krypton isotherms.*[1] However, solid oxide fuel cell (SOFC) electrodes are sintered ceramic oxides for which both average particle size and mass of material are relatively low, especially for laboratory-scale samples. Typical electrode specific surface areas are ~ 1-10 m^2/g, which for lab-scale electrode masses will result in only 0.01-0.1 m^2. BET setups also have the disadvantage that the dimensions of the tube usually constrain the sample to be no larger than 1 cm in width. As a result, BET methods have not been widely applied to characterize SOFC electrodes.

Nonetheless, surface area is an important parameter determining electrode performance: for MIEC materials, the Adler-Lane-Steele model shows a direct relationship between polarization resistance and surface area,[2] whereas for composite electrodes, three-phase boundary density can be related directly to particle size and hence surface area.[3] Full explorations of the structure-property-performance relationship have been conducted for a wide variety of SOC materials but usually involve time-intensive tomographic methods, such as focused ion beam (FIB)-assisted scanning electron microscopy (SEM) or synchrotron X-ray computed nanotomography (nano-CT). The result of either is a 3D-reconstruction stitched from interpolated 2D images with extensive

* For example, in the Micromeritics 3Flex analyzer with 12mm tubes, >1.55 m^2 is needed for <1% uncertainty and >0.3 m^2 is needed for <5% uncertainty

microstructural information, but neither can resolve the features found in solid oxide cells incorporating infiltrated or exsolved nanoparticles. FIB-SEM offers the better voxel size of ~30 nm, which requires particle sizes to be ~450 nm for error to be <5%. This poses a problem for nanostructured hierarchical systems; for example particles infiltrated on a scaffold can be <50 nm and some metal exsolution systems give rise to particles as small as 5 nm.[4] Another technique, mercury porosimetry, can allow approximate surface area to be calculated from a distribution of cylindrical pore sizes based on the pressure needed to infiltrate such pores; this prescribed form factor, however, is not conducive to measuring irregular and/or nanoparticle-decorated surfaces.

Here we demonstrate a new method for accurately measuring surface areas of samples with net areas of 1-1000 cm^2. The method is conceptually similar to the controlled nitrogen physisorption used in BET to extract surface area, but instead uses self-limiting adsorption of ALD chemical precursors alongside chemical analysis. In this methodology, a fast, direct 200°C ALD alumina process is demonstrated. With a well-calibrated thickness per ALD cycle, *n* number of cycles results in a known layer thickness. The volume of the ALD deposit is then ascertained either gravimetrically (via the known density of the ALD layer) or, more sensitively, from digesting the alumina overcoat and measuring concentration via inductively coupled plasma emission spectroscopy (ICP-OES). The known volume is divided by the known thickness to result in an absolute surface area. Finally, specific surface area is obtained by dividing by the known total mass or volume. Examples of the application of the technique to SOFC electrodes are presented, and advantages and limitations are discussed. The method can determine low absolute surface areas (~1 cm^2) of meso/macroporous structures (pore radius > 6 nm), including those with nanoscale features.

Experimental Methods

Solid Oxide Fuel Cell and Electrode Preparation

Symmetric oxygen electrode cells and symmetric fuel electrode cells were prepared similarly. In the case of oxygen electrodes, the Gd-doped ceria electrolyte was prepared via pellet pressing of ultra-high surface area $Gd_{0.1}Ce_{0.9}O_{1.95}$ powder (Rhodia) using 1.5 metric tons of pressure and were fired at 1450°C for 6 hours. A composite ink of $(La_{0.8}Sr_{0.2})_{0.98}MnO_{3-\delta}$ (LSM) (Praxair) with 50/50 wt% GDC (LSM/GDC) was 3-roll milled with Heraeus V-737 binder in a weight ratio of 1:1.18 binder, and then screen-printed onto either side of the GDC electrolyte and fired at 1250°C for 4 hours. Praseodymium oxide infiltration solutions of 2M in water were created from Pr-nitrate hexahydrate and citric acid as a chelating agent,[5] and were pipetted into the electrodes, which were then calcined at 450°C.

Fuel electrodes were prepared atop commercial scandia-stabilized zirconia (ScSZ) electrolyte pellets of ~200 μm thickness (Fuel Cell Materials, Hionic™), later printed with a Gd-doped ceria barrier layer ink in-house. Solid state synthesis of $SrCO_3$ (Aldrich), TiO_2 (Aldrich), Fe_2O_3 (Alfa Aesar), and $Ni(NO_3)_2 * 6H_2O$ (Strem) was conducted at 1200°C in air following the protocol in Zhu et al.[6] to form three compositions: $Sr_{0.95}(Ti_{0.3}Fe_{0.63}Ni_{0.07})O_{3-\delta}$ ($S_{0.95}$TFN), $Sr(Ti_{0.3}Fe_{0.63}Ni_{0.07})O_{3-\delta}$ ($S_{1.00}$TFN), and $Sr(Ti_{0.3}Fe_{0.7})O_{3-\delta}$ (STF).[6] The powders were ball-milled pre- and post- calcination for 4 days in ethanol. The powder was then combined with Heraeus V-737 vehicle with a ratio of 1:1.2 powder-to-vehicle and processed through a 3-roll mill to produce an ink. This ink was then screen-printed and the cells fired at 1150°C in air for 3 hours.

Scanning electron microscopy and energy dispersive spectroscopy (SEM/EDS) took place in a Hitachi SU8030 with an Oxford AZtec X-max 80 SDD. Prior to imaging, samples were fractured and then plasma-coated with ~9 nm osmium for conductivity (OPC). Brunauer–Emmett–

Teller (BET) gas adsorption isotherm theory was used to obtain extra surface area information with a Micromeritics 3Flex instrument using krypton gas; here, enough electrode sample was generated for the measurement (> 1 m^2) by drying and firing an unusually large amount of LSM/GDC composite ink. Electrode mass was determined via a Mettler Toledo UMX2 microbalance with a sensitivity of 0.1 µg.

Al_2O_3 Atomic layer deposition

An overview of the steps involved in the surface area determination appears in Figure 1. ALD was carried out using an Arradiance GEMstar-8 ALD system with trimethylaluminum (TMA) and water vapor. To coat the electrodes on both sides of the symmetric cells, samples were either placed in a metallic mesh bag or suspended via a clip. After pumping down to low vacuum (~30 mTorr) via roughing pump, the samples were allowed to equilibrate at 200°C for 10 minutes. The ALD process used an exposure mode with in which the actuator out of the chamber was closed for 1.5 s after an 11 ms pulse of precursor, then opened for 1 s. Operating in exposure mode allows for greater diffusion time for the precursor through porous structures.[7] These exposures were repeated four times for a combined 8.5 seconds of dosage per precursor, then purged for 20 seconds, followed by the same process for water, for a total of 50 precursor/oxidant cycles. At approximately 1.25 Å/cycle,[8] a total thickness of 6.25 nm was deposited. A version of the recipe with 22 ms doses was also used and it resulted in the same amount of alumina, so 11 ms was determined to be a saturating dose.

Surface Area Determination

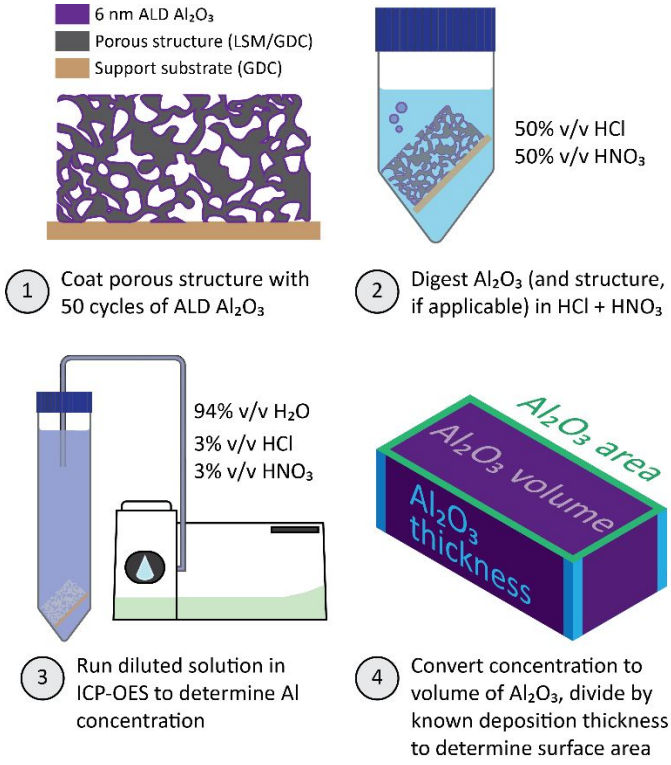

Figure 1. Process overview for the surface area determination technique using ALD and ICP-OES.

After coating, the cells were placed in 1:1 HCl:HNO_3 solution of 0.72 mL and left for 24 h without agitation or heat. Hydrochloric acid has previously been shown to be able to dissolve perovskite SOFC electrodes.[9, 10] Nitric acid is a well-known solvent for nickel and other metals, and together as aqua regia they are capable of dissolving noble metals. The ceria components of the cells do not dissolve and were left in the tubes in order to prevent possible contamination from retrieval. After 24 h, the solution was diluted to be 3%/3% HCl/HNO_3 in ultrapure water.

ICP-OES was conducted on a Thermo iCAP 7600 ICP-OES. Standards were prepared using serial dilution of a combined elemental standard from 100 to 0.01 ppm. The samples were run in radial mode, analyzing for constituent electrode elements as well as aluminum. Several emissions lines for each element were chosen, selecting for ones without interference from other

known elements, and the instrument took measurements in triplicate; the ultimate emission line chosen was that with the lowest standard deviation. Data was analyzed by converting from concentration (mass basis) to mass by multiplying by the total mass of the solution in the tube (1.0207 g/mL * 12 mL = 12.2484 g), and then to moles by dividing by the atomic weight per mole of the element. For aluminum, the volume is obtained by dividing the mass by the density of Al_2O_3 – for an ALD process at a similar 177°C, this was found to be 3.0 g/cm^3.[8] The surface area can then be obtained by dividing the volume by the known deposition thickness. For 50 cycles, at 1.25Å/cycle,[8] this is 6.25 nm. Note that the exact growth-per-cycle is non-uniform for the first ~20 cycles,[11] so this value is expected to overestimate the height of the ALD layer and thus underestimate the surface area. Comparison with a BET measurement from a large-area specimen allowed for a more precise calibration of the thickness: 1.19 Å/cycle. In some cases, if the contribution to the surface area from the electrolyte supports was thought to be significant, image analysis was used to subtract those areas using images of the cells taken before acid digestion. In the LSM/GDC samples, this contribution was ~1% and determined to be negligible, but for the lower absolute surface area STF(N) samples, contributions were ~10% and were therefore subtracted. Finally, surface area can be normalized on a per-mass basis using the ICP-OES derived mass of the electrode, since it too is dissolved in the acid matrix, thus allowing for a complete picture of chemical composition, mass, and surface area.

Validation

To determine the accuracy of the technique, several outstanding questions need to be answered, concerning whether the Al_2O_3 coating fully dissolves in the modified aqua regia, whether the coating is uniform, if it is subject to diffusional limitations, and whether the data is comparable to results from BET analysis.

Because ALD processes can yield non-uniform coverage in some cases, especially with high aspect ratio structures, the penetration depth of the ALD process was measured.[7, 10] In previous studies with a Zr-based ALD precursor, the Zr signal was tracked into a porous solid via cross-sectioning and SEM-EDS analysis for chemical mapping.[10] Similar results are shown in Figure 2 for two cells—an infiltrated LSM/GDC sample with higher specific surface area and of ~17 μm thickness, and a Ni/yttria-stabilized zirconia (Ni/YSZ) composite electrode of ~300 μm thickness.

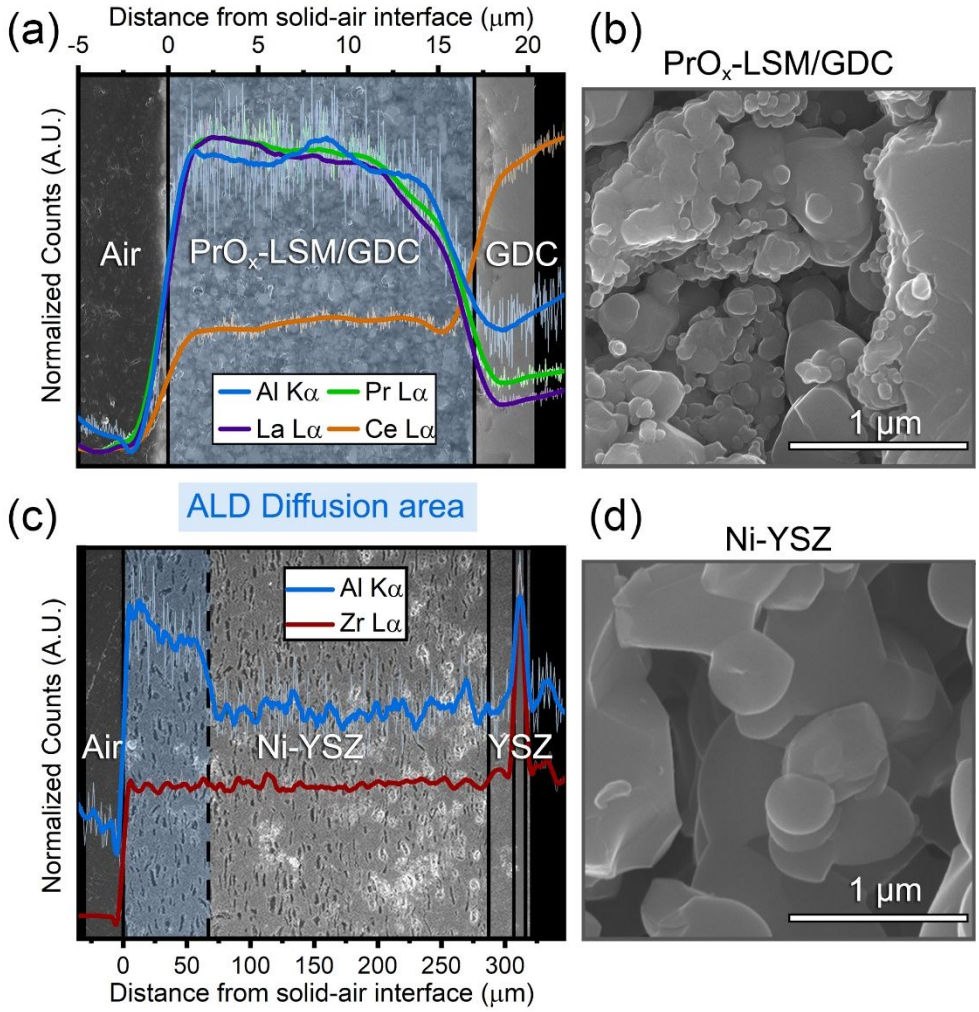

Figure 2. Tracking the signal of Al diffused into porous electrode scaffolds by SEM/EDS line-scan, with (a) and (b) depicting an EDS linescan and magnified morphology of an infiltrated oxygen electrode, PrOx-LSM/GDC, and the bottom (c) and (d) the same for a Ni/YSZ support. Line-scans were conducted on epoxy-infiltrated and polished cross-sections, while magnified views were on fractured cross-sections to show 3-dimensional features.

In Figure 2(a), the Al signal can be seen tracking with representative elements of the scaffold, namely Pr representing the infiltrated species, La representing the LSM, and Ce representing the GDC. Here, the microstructure has features <100 nm, typical of low temperature solid oxide cell electrodes. The Ni/YSZ tape-casted support layer shown in Figure 2(c) is much thicker and hence provides a case with very long aspect ratio pores. The aluminum signal falls off after about 50 μm into the scaffold, indicating a diffusion limit was reached. A conservative

estimate from the EDS scans is that the ~10 s half-cycles used are sufficient for up to 50 μm depths in the case of the Ni-YSZ. Given Knudsen diffusion depth is related to $t^{1/2}$,[12] the thinner LSM/GDC scaffold should have only required 1.2 s of diffusion time, and the much thicker Ni/YSZ would require 360 s or 6 minutes of exposure, assuming similar aspect ratio pores.

A second set of validations was done to benchmark the ALD/ICP-OES measured surfaces areas against ALD weight gain measurements and BET measurements. In the former, the difference in sample weight before and after alumina deposition is used to generate the mass of deposited species. The mass generated from this method and the mass from the concentration measured from ICP-OES are compared and fall very close together (Figure 3), except with a larger standard deviation arising from the mass-based method. This is strong evidence that the alumina overcoat is digested in the HCl:HNO_3 acid matrix used for the ICP-OES measurement.

To allow a direct comparison of BET versus ALD/ICP-OES, an adequately large amount of LSM/GDC ink that was used for the cells was fired and formed a self-supported scaffold, shown in Figure S1. Two samples, of mass 1.06 g and 1.03 g, were used with expected errors of <0.77% given their absolute surface areas according to the equipment manufacturer's specifications.[1] The BET surface areas were ~7% higher than those estimated by ALD (Figure 3). If we assume that BET provides the true surface area, then the ALD GPC value can be adjusted accordingly. This BET-calibrated GPC, assuming the same ALD alumina density of 3.0 g/cm^3, is 1.19 Å/cycle, or 95.2% of the reported 1.25 Å/cycle value.[8] This adjustment is not surprising given that the reported GPC is a steady-state value, whereas the first ~20 cycles of ALD Al_2O_3 are known to produce an impeded growth rate with Volmer-Weber islands, arising from the higher interfacial energy between the deposited oxide and the substrate.[11]

To estimate the noise floor of the measurement, identical samples prepared without an ALD overlayer were also measured and resulted in specific surface areas of 0.09±0.06 m^2/g (Figure 3); these values are a combination of the instrument noise with trace Al impurities in the electrode materials and solvent, and align well with the standard deviations noted in the coated samples.

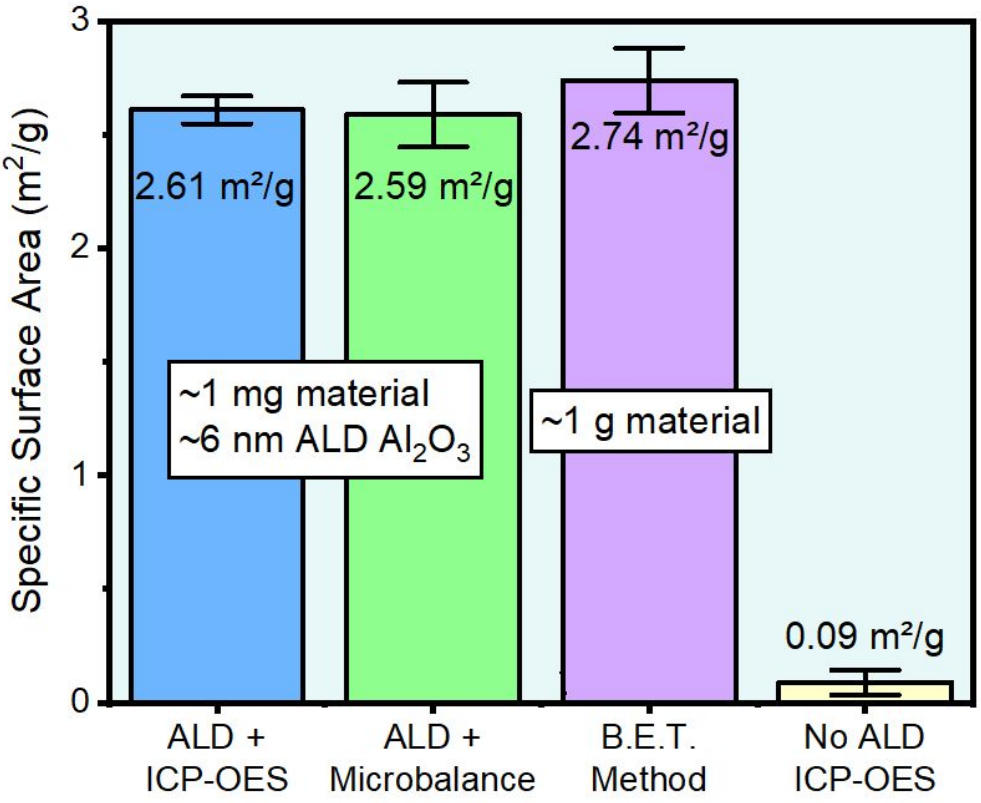

Figure 3. Comparison between methodologies of surface area determination, two using the ALD method (one deriving Al_2O_3 volume by ICP-OES, the other by its mass) and the last using the BET method. Also shown is the signal and error from ICP-OES on samples that were not coated with ALD-Al_2O_3.

Examples of the technique

Below, the novel surface area technique is used in two examples to demonstrate its applicability in solid oxide cell development.

Coarsening of Electrode with Infiltrated PrO_x

Infiltrated SOFC electrodes have internal surfaces coated with nanoparticles that are known to initially increase surface area but which coarsen during extended elevated-temperature operation.[13] Although these nanoparticles can sometimes be discerned by electron microscope observations, it is difficult to estimate their size or surface area as well as changes due to their coarsening. In previous work with an infiltrated PrO_x system, scanning transmission electron microscopy with EDS highlights the qualitative microstructural contribution from the infiltrated species; [5] however, from micrographs alone it is difficult to assign a bulk value of surface area increase.

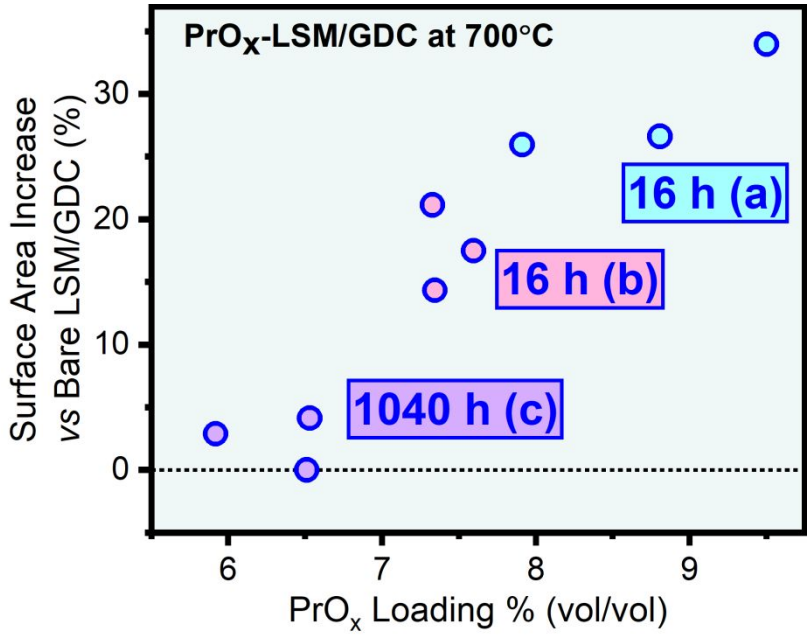

Figure 4. Increase in surface area relative to bare LSM-GDC (2.7 m^2/g) as measured by the ALD surface area technique. Two samples (a) and (b) with limited ageing (16 h at 700°C) show a wide

disparity in PrO_x loading which is linearly related to the surface area increase. After 1 kh (c), the surface area increase of another sample has been reduced by coarsening.

For this example application, LSM/GDC was infiltrated with PrOx nanoparticles and surface area was determined using this paper's method, both early into a 700°C annealing period (16 h) and later (1040 h). An advantage of this method is that secondary chemical information such as species loading can be determined, in this case Pr-loading (volume percent occupied by the additional phase versus total volume of the electrode). The increase in surface area versus the bare LSM/GDC is shown as the y-axis in Figure 4, with the corresponding loading of PrO_x on the x-axis. First, it is apparent by the two 16 h samples that the amount of PrO_x loaded into the cells was highly variable. Samples marked (a) and (b), cells prepared identically, showed a range of Pr-content from about 7.5 to 9.5%; each cell was broken into 3 and the ICP-measured fragments are shown as individual data points – they too vary despite being from the same cell. This is not surprising given only one round of infiltration was used and given the imperfect wetting behavior of nitrate solutions into oxides. The sample measured after 1040 h of coarsening shows lower Pr loading, but its surface area increase over bare LSM/GDC was very minimal, in one sample even slightly negative. This result points to a nearly full negation of any surface area increase due to coarsening after 1000 h operation at 700°C. Micrographs of the samples are shown in Figure S2.

Exsolution of Metal Particle Decorations

Exsolution of nanoparticle catalysts from oxide surfaces is a method for enhancing solid oxide fuel electrode performance.[14, 15] Such nanoparticles should substantially increase the net electrode surface area and allow for quantification of the extent and morphology of nanoparticle formation, but heretofore only BET surface area analysis of bulk powders has been conducted.[16, 17] Here we explore sintered STF and STFN fuel electrodes in which Fe or bimetallic Ni-Fe exsolution respectively, has been observed.[6, 18] Figure 5 illustrates the change in the electrode

surface morphology before and after exsolution in SEM images for the three compositions: $Sr(Ti_{0.3}Fe_{0.7})O_{3-\delta}$ (STF), $Sr(Ti_{0.3}Fe_{0.63}Ni_{0.07})O_{3-\delta}$ ($S_{1.00}$TFN), and $Sr_{0.95}(Ti_{0.3}Fe_{0.63}Ni_{0.07})O_{3-\delta}$ ($S_{0.95}$TFN).

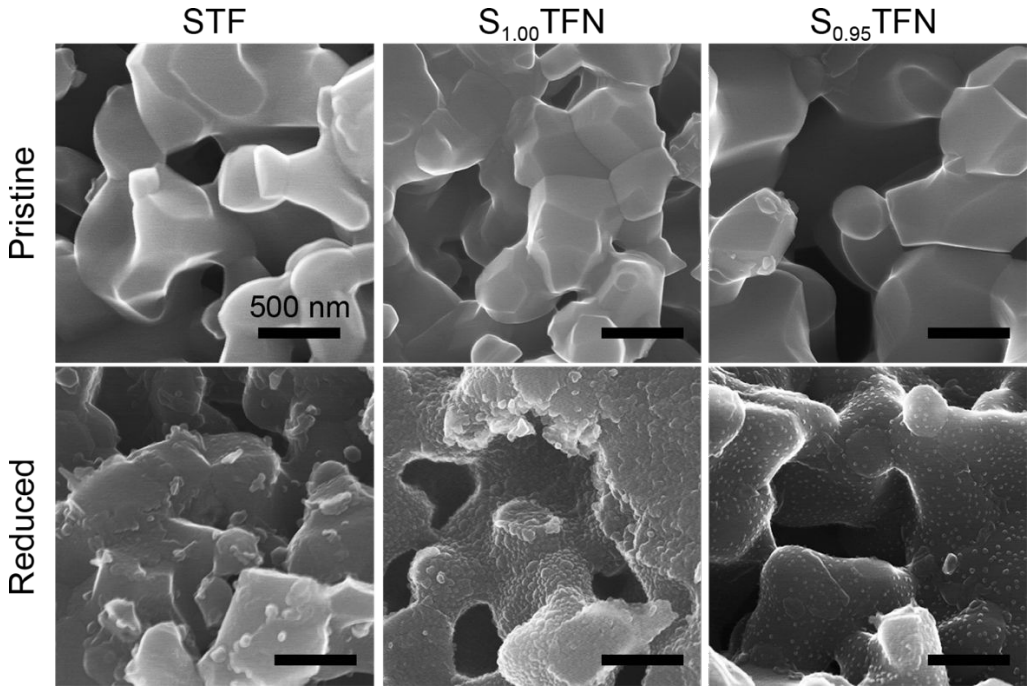

Figure 5. SEM images of (a) STF and (b) reduced STF, (c) $S_{1.00}$TFN and (d) reduced $S_{1.00}$TFN, and (e) $S_{0.95}$TFN and (f) reduced $S_{0.95}$TFN. All scale bars 500 nm.

Figure 6 shows surface areas measured using the ALD/ICP-OES method for each of the oxides. In each case, there is an original, pre-reduction (pristine) surface area measured, and an increase in area due to reduction-induced exsolution; the largest gain in surface area comes from the stoichiometric $S_{1.00}$TFN system which seems to nucleate a crowded, packed array of hemispherical particles. STF nucleates many larger, more fully spherical Fe particles and has the largest absolute surface area. The exsolution in A-site deficient $S_{0.95}$TFN is the least extensive and a lower areal density of (Ni,Fe) particles is apparent. This lower particle density allows for a reasonable estimate to be made, in this case, about 400 particles per μm^2, a surface area increase

of 17.7% corresponds to a 23.7 nm hemisphere, close to the average of 21.9±6.3 (median, 21.3) from image analysis.

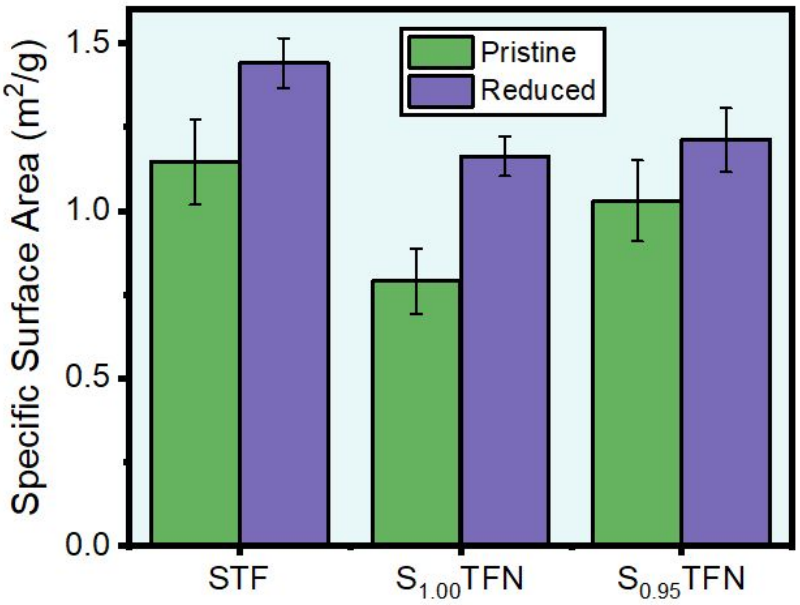

Figure 6. ALD-derived surface areas for STF, stoichiometric $S_{1.00}$TFN, and A-site deficient STFN ($S_{0.95}$TFN).

Discussion

Previously, ALD combined with emission spectroscopy has been used on materials of known surface area to estimate the effectiveness of the ALD process in cohesively covering the sample—our methodology sees this process in reverse, leveraging the prototypical ALD precursor, trimethylaluminum (TMA). The TMA-water process is nearly ideal in that (1) both precursors are stable enough to avoid excessive thermal decomposition but are reactive enough with each other (2) they are of high vapor pressure, and (3) their reaction product, methane, is inert with either of them at deposition conditions.[7] TMA has been used to coat high aspect ratio anodic TiO_2 nanotubes with aspect ratios of ~180 with precursor exposure times of 4-5 seconds to ensure enough diffusion time is available.[19] This aspect ratio is similar to SOFC electrodes of pore diameters >100 nm and <20 μm thick, resulting in aspect ratios <200.[10] Due to the robustness of TMA, exposure times even in excess of 10 s result in stable growth rates. Therefore, the TMA/water process is robust enough that results should be reproducible with many kinds of reactors and slight process deviations. One potential constraint to using TMA to deposit Al_2O_3 is if the porous structure itself contains aluminum; in this event, ZnO deposited via diethyl zinc (DEZ)/H_2O may be a suitable oxide alternative and has been demonstrated to to stably coat high aspect ratio structures up to L/d ~5000.[20] Titania via $TiCl_4/H_2O$ may be another that could fit this metholodogy. A previous protocol study used ALD-TiO_2 in conjunction with dye adsorption and UV-vis to estimate surface areas, as is common in the dye-sensitized solar cell field, but such a measurement is less direct on account of the dye intermediary and involves a prohibitive 500°C annealing step (risking reactions with many substrates) to favor a particular TiO_2 crystallographic plane.[21]

Here, the alumina overcoat was shown to be fully dissolved in 1:1 hydrochloric to nitric acid by calculating the weight per sample of Al_2O_3 from the ICP-OES measurement and comparing

to the weight gain from a microbalance, allowing for a much more precise measurement of concentration. The ALD-derived surface area calculated using literature values of growth-per-cycle and density is within 6% of the "gold standard" measurement technique, BET analysis, but with milligram quantities of electrode material needed, rather than gram quantities. It therefore pairs well with the quantities used in standard button-cell testing of ceramic electrochemical materials. Of course, it can also be applied to large-area cells by cutting samples with size consistent with ALD and ICP-OES sample chambers. ICP-OES can be used to quantify electrode chemical concentrations, such as the volume loading of an infiltrated species, and comparison to un-infiltrated electrodes allows for a better understanding of the morphological changes upon infiltration.

Greater or lesser surface area samples can be measured by this technique. Coated samples in this study had measured Al concentrations from 2-10 ppm, sufficiently larger than the experimentally measured noise floor of ~70 ppb, an error that includes the radial mode detection limit of Al at ~50 ppb as well as any impurities in the samples/solution.[22] An ALD cycle number of 50 (~6 nm) was selected to provide adequate concentration of Al in solution while avoiding clogged mesopores, but greater thicknesses could be deposited to increase concentration in the event of a more open pore structure. Sensitivity could be improved by ~10x by running the ICP-OES in axial mode, but this can be at the cost of decreased precision due to greater matrix interferences.[23] Therefore, samples of lower absolute surface area can be measured so long as concentration exceeds the noise floor specific to the setup, which can be defined by analyzing samples prepared without ALD overcoats. This applies further to ICP-MS (mass spectroscopy) with an Al detection limit of 30 ppt; here, care must also be taken to limit the solution's total dissolved solids to an accepted <0.2% versus the accepted <10% for ICP-OES. For the upper limit

of sample surface area, ICP-OES standards are commonly available up to 1% which is 1,000 times greater than the concentrations measured here, and would result in surface areas far greater than could be reasonably achieved by sintered ceramic electrodes.

Therefore, subject to the above constraints of thickness, pore size, and chemical composition, this technique measures a range of surface areas relevant to the development of sintered ceramic electrodes with specific surface areas on the order of 0.1-50 m^2/g. The technique is relatively accessible; many universities possess both ALD and ICP-OES in user facilities, and the hands-on time is low, with each technique running largely automatically. At the time of writing, the per-hour institutional rate at the authors' institution was $33 and $72, respectively (commercial rates $66 and $180, respectively), with total cost for a batch of measurements at around $130. Due to its ease of use versus other surface area determination methods and its pairing with an established analytical chemistry method, the technique enables a useful combined chemical/morphological approach to characterization of next-generation solid oxide electrode performance, and may find other uses in the broad field of heterogeneous catalysis.

Acknowledgements

The authors gratefully acknowledge financial support by the Department of Energy Basic Energy Sciences, grant # DE-SC0016965. This work made use of the EPIC and NUFAB facilities of Northwestern University's NUANCE Center, which has received support from the SHyNE Resource (NSF ECCS-2025633), the IIN, and Northwestern's MRSEC program (NSF DMR-1720139). Metal analysis was performed at the Northwestern University Quantitative Bio-element Imaging Center, for which R. Sponenburg is thanked. This work also made use of the IMSERC Physical Characterization facility at Northwestern University, which has received support from the Soft and Hybrid Nanotechnology Experimental (SHyNE) Resource (NSF ECCS-2025633), and Northwestern University. Gas isotherm measurements were performed at the REACT Core Facility at Northwestern University, supported by a grant from the DOE (DE-SC0001329).

References

1. I. Micromeritics, Tech Tip 14: Minimum Surface Area Measurements with micromeritics Physisorption Analyzers.*Journal*.
2. S. B. Adler, J. A. Lane and B. C. H. Steele, Electrode Kinetics of Porous Mixed-Conducting Oxygen Electrodes, *Journal of The Electrochemical Society*, 1996, **143**, 3554-3564.
3. M. Mogensen and S. Skaarup, Kinetic and geometric aspects of solid oxide fuel cell electrodes, *Solid State Ionics*, 1996, **86-88**, 1151-1160.
4. R. Glaser, T. Zhu, H. Troiani, A. Caneiro, L. Mogni and S. Barnett, The enhanced electrochemical response of Sr(Ti0.3Fe0.7Ru0.07)O3-delta anodes due to exsolved Ru-Fe nanoparticles, *J Mater Chem A*, 2018, **6**, 5193-5201.
5. M. Y. Lu, R. Scipioni, B.-K. Park, T. Yang, Y. A. Chart and S. A. Barnett, Mechanisms of PrOx performance enhancement of oxygen electrodes for low and intermediate temperature solid oxide fuel cells, *Materials Today Energy*, 2019, **14**, 100362.
6. T. L. Zhu, H. E. Troiani, L. V. Mogni, M. F. Han and S. A. Barnett, Ni-Substituted Sr(Ti,Fe)O-3 SOFC Anodes: Achieving High Performance via Metal Alloy Nanoparticle Exsolution, *Joule*, 2018, **2**, 478-496.
7. T. M. Onn, R. Kungas, P. Fornasiero, K. Huang and R. J. Gorte, Atomic Layer Deposition on Porous Materials: Problems with Conventional Approaches to Catalyst and Fuel Cell Electrode Preparation, *Inorganics*, 2018, **6**, 34.
8. M. D. Groner, F. H. Fabreguette, J. W. Elam and S. M. George, Low-temperature Al2O3 atomic layer deposition, *Chemistry of Materials*, 2004, **16**, 639-645.
9. H. Wang, K. J. Yakal-Kremski, T. Yeh, G. M. Rupp, A. Limbeck, J. Fleig and S. A. Barnett, Mechanisms of Performance Degradation of (La,Sr)(Co,Fe)O3-δSolid Oxide Fuel Cell Cathodes, *Journal of The Electrochemical Society*, 2016, **163**, F581-F585.
10. T. A. Schmauss, J. G. Railsback, M. Y. Lu, K. Y. Zhao and S. A. Barnett, ZrO2 atomic layer deposition into Sr0.5Sm0.5CoO3-delta-Ce0.9Gd0.1O2-delta solid oxide fuel cell cathodes: mechanisms of stability enhancement, *J Mater Chem A*, 2019, **7**, 27585-27593.
11. R. L. Puurunen, W. Vandervorst, W. F. A. Besling, O. Richard, H. Bender, T. Conard, C. Zhao, A. Delabie, M. Caymax, S. De Gendt, M. Heyns, M. M. Viitanen, M. de Ridder, H. H. Brongersma, Y. Tamminga, T. Dao, T. de Win, M. Verheijen, M. Kaiser and M. Tuominen, Island growth in the atomic layer deposition of zirconium oxide and aluminum oxide on hydrogen-terminated silicon: Growth mode modeling and transmission electron microscopy, *Journal of Applied Physics*, 2004, **96**, 4878-4889.
12. T. Keuter, G. Mauer, F. Vondahlen, R. Iskandar, N. H. Menzler and R. Vaßen, Atomic-layer-controlled deposition of TEMAZ/O2–ZrO2 oxidation resistance inner surface coatings for solid oxide fuel cells, *Surface and Coatings Technology*, 2016, **288**, 211-220.
13. A. V. Call, J. G. Railsback, H. Wang and S. A. Barnett, Degradation of nano-scale cathodes: a new paradigm for selecting low-temperature solid oxide cell materials, *Phys Chem Chem Phys*, 2016, **18**, 13216-13222.
14. T. Cao, O. Kwon, R. J. Gorte and J. M. Vohs, Metal Exsolution to Enhance the Catalytic Activity of Electrodes in Solid Oxide Fuel Cells, *Nanomaterials (Basel)*, 2020, **10**.
15. C. Tang, K. Kousi, D. Neagu and I. S. Metcalfe, Trends and Prospects of Bimetallic Exsolution, *Chemistry*, 2021, **27**, 6666-6675.

16. Y. F. Sun, Y. Q. Zhang, J. Chen, J. H. Li, Y. T. Zhu, Y. M. Zeng, B. S. Amirkhiz, J. Li, B. Hua and J. L. Luo, New Opportunity for in Situ Exsolution of Metallic Nanoparticles on Perovskite Parent, *Nano Lett*, 2016, **16**, 5303-5309.
17. A. Donazzi, T. A. Schmauss and S. A. Barnett, Catalytic and electrocatalytic performance of Sr(Ti0.3Fe0.7Ru0.07)O3-δ for applications in solid oxide fuel cells supplied with ethanol steam reforming mixtures, *J Power Sources*, 2022, **551**, 232215.
18. M. Santaya, C. E. Jiménez, H. E. Troiani, E. A. Carbonio, M. D. Arce, L. M. Toscani, R. Garcia-Diez, R. G. Wilks, A. Knop-Gericke, M. Bär and L. V. Mogni, Tracking the nanoparticle exsolution/reoxidation processes of Ni-doped SrTi0.3Fe0.7O3−δ electrodes for intermediate temperature symmetric solid oxide fuel cells, *J Mater Chem A*, 2022, **10**, 15554-15568.
19. R. Zazpe, M. Knaut, H. Sopha, L. Hromadko, M. Albert, J. Prikryl, V. Gartnerova, J. W. Bartha and J. M. Macak, Atomic Layer Deposition for Coating of High Aspect Ratio TiO2 Nanotube Layers, *Langmuir*, 2016, **32**, 10551-10558.
20. J. W. Elam, D. Routkevitch, P. P. Mardilovich and S. M. George, Conformal Coating on Ultrahigh-Aspect-Ratio Nanopores of Anodic Alumina by Atomic Layer Deposition, *Chemistry of Materials*, 2003, **15**, 3507-3517.
21. S. M. Ubnoske, Q. Peng, E. R. Meshot, C. B. Parker and J. T. Glass, Protocol for High-Sensitivity Surface Area Measurements of Nanostructured Films Enabled by Atomic Layer Deposition of TiO2, *The Journal of Physical Chemistry C*, 2015, **119**, 26119-26127.
22. P. R. Gaines, *ICP Periodic Table Guide*, Inorganic Ventures, 2017.
23. G. Tyler and S. Jobin Yvon, ICP-OES, ICP-MS and AAS Techniques Compared, *ICP Optical Emission Spectroscopy Technical Note*, 1995, **5**.